Manipulating the Gibberellin Pathway Alters Harvest Index and Cannabinoid Content in *Cannabis sativa* L.

Lennard Garcia-de Heer, Matthew Nolan, Jos Mieog, Qi Guo, Nicolas Dimopoulos, Lei Liu, Xuan Chen, Tobias Kretzschmar

Manipulating the Gibberellin Pathway Alters Harvest Index and Cannabinoid Content in *Cannabis sativa* L.

Running head: Manipulation of gibberellins in *Cannabis sativa* L.

Corresponding Author: T Kretzschmar; Faculty of Science and Engineering/Southern Cross University/ 1 Military Rd Lismore/ NSW/ 2480/ Australia/ tobias.kretzschmar@scu.edu.au

Subject areas – Growth and development, Regulation of gene expression

Black and white figures: 2

Colour figures: 5

Tables: 0

Supplementary Figures: 8

Supplementary Tables: 16

Manipulating the Gibberellin Pathway Alters Harvest Index and Cannabinoid Content in *Cannabis sativa* L.

Running head: Manipulation of gibberellins in *Cannabis sativa* L.

Lennard Garcia-de Heer[1], Matthew Nolan[1], Jos Mieog[1], Qi Guo[1], Nicolas Dimopoulos[1], Lei Liu[1], Xuan Chen[2], Tobias Kretzschmar[1*]

[1]Faculty of Science and Engineering, Southern Cross University, Lismore, NSW 2480, Australia

[2]Industrial Crops Research Institute, Yunnan Academy of Agricultural Sciences, Kunming 650205, China

[*] Corresponding Author: tobias.kretzschmar@scu.edu.au

Lennard Garcia-de Heer: l.garcia-de.heer.12@student.scu.edu.au

0009-0009-2929-3357

Matthew Nolan: m.nolan.14@student.scu.edu.au

0009-0000-1314-0297

Jos Mieog: jos.mieog@scu.edu.au

0000-0002-2153-8956

Qi Guo: qi.guo@scu.edu.au

0000-0002-3528-2533

Nicolas Dimopoulos: nicolas.dimopoulos@scu.edu.au

0000-0002-5352-5674

Lei Liu: ben.liu@scu.edu.au

0000-0002-3710-7042

Xuan Chen: chenxuan9239@163.com

0009-0004-4333-1376

Tobias Kretzschmar: tobias.kretzschmar@scu.edu.au

0000-0002-8227-0746

Abstract

Cannabis sativa is a multi-purpose crop with a wide range of industrial and medicinal end uses. Despite its long history of cultivation, it has not received the same breeding efforts as many other crops due to regulatory barriers. In particular, it bypassed the Green Revolution, which improved harvest indices of crops via developing semi-dwarf varieties by manipulating endogenous gibberellin signalling pathways. We chemically manipulated gibberellin signalling through the exogenous application of gibberellic acid and the gibberellin biosynthesis inhibitor paclobutrazol. We used multi-omic analysis to determine the effect of these applications on the proteome, transcriptome and secondary metabolite accumulation to assess the potential of gibberellin

modulation for improved *C. sativa* end uses. Paclobutrazol treatments resulted in a semi-dwarf phenotype with an improved high harvest index and enhanced cannabinoid accumulation. Differentially expressed gene and weighted gene co-expression network analysis revealed the importance of source/sink dynamics for harvest index, with the increased expression of sucrose synthases and sugar transporters key to the phenotypic changes induced by gibberellin modulation. At the same time, the availability of hexanoate precursors via the degradation of long-chain fatty acids emerged as a likely constraint on cannabinoid accumulation. This study provides a basis for exploring the manipulation of gibberellin pathways in *C. sativa* varieties and their relevance to cannabinoid production.

Keywords
Harvest index, resource allocation, Green Revolution, secondary metabolite, semi-dwarf, source/sink dynamics

Abbreviations
ABA – Abscisic acid

CBCA- cannabichromenic acid

CBDA – cannabidiolic acid

CBDVA - Cannabidivarinic acid

CBGA - cannabigerolic acid

DAP – differentially abundant proteins

DEG – differentially expressed genes

GA – gibberellins

GA_3 – gibberellic acid

GA3 – Experimental treatment group

GAox – Gibberellin oxidase

JA – jasmonates

PBZ – paclobutrazol

SWATH – sequential window acquisition of all theoretical mass spectra

THCA – tetrahydrocannabinolic acid

Introduction

Cannabis sativa is a predominantly dioecious species with a long history of human cultivation for diverse products (Garcia-de Heer et al., 2024; McPartland et al., 2019). These include psychoactive cannabinoids from female flowers for recreational and therapeutic use, seeds rich in polyunsaturated fatty acids for consumption, bast fibre for textiles, and, more recently, hurd for construction and biofuel (Schluttenhofer & Yuan, 2017). The psychoactive properties of the female flowers prompted nearly a century of prohibition (Johnson, 2019). Glandular trichomes on female flowers store a wide array of bioactive terpenoids and cannabinoids. Terpenoids are synthesised via the plastidial 2-C-methyl-D-erythritol 4-phosphate (MEP) or the cytosolic mevalonic acid (MVA) pathways. Cannabinoids arise from condensation of MEP pathway-derived geranyl diphosphate (GPP) and olivetolic acid (OLA), produced through the cytosolic polyketide pathway, to form the fundamental cannabinoid cannabigerolic acid (CBGA), before being cyclised by terminal synthases to produce the end

product cannabinoids such as tetrahydrocannabinolic acid (THCA) and cannabidiolic acid (CBDA) (Andre et al., 2016). Recognition of cannabinoid therapeutic potential has eased regulatory barriers, fuelling rapid growth of the medicinal cannabis industry. However, prolonged prohibition limited advances in breeding and production that have transformed yields in other crops over the past century (Pingali, 2012). Given high demand for its products and substantial genetic diversity, *C. sativa* is well placed to apply modern agricultural innovations to accelerate the improvement of this ancient crop (McPartland & Small, 2020).

The yield gains of the 1960s 'Green Revolution' arose from newly available agrochemicals and the introduction of high-yielding semi-dwarf rice and wheat (Hazell, 2009). Semi-dwarf varieties are more resistant to lodging, decreasing yield loss and altered resource partitioning, increasing harvest index (HI) by directing biomass from vegetative tissue to reproductive organs. Semi-dwarfism is now a key agronomic trait in many crops (Morikawa et al., 2007; Robinson, 2011). Although high-HI semi-dwarf (HHISD) wheat and rice were bred independently, both arose from altered gibberellin (GA) signalling (Hedden, 2003). HHISD *C. sativa* varieties have been proposed to boost seed and cannabinoid yields (Small, 2018), whereas low-HI forms may benefit fibre and hurd production. Manipulating GA signalling is therefore a logical breeding target. While the genetic basis of HI is well defined in cereals, its application to an emerging multi-purpose crop such as *C. sativa* remains largely unexplored.

GAs are diterpenoid carboxylic acids with diverse functions in higher plants, including seed germination, maturation, flowering, and reproductive development (Hedden & Sponsel, 2015). GAs act by removing growth-limiting factors, most notably promoting cell elongation to increase internode length, and act antagonistically with jasmonates (JA) or abscisic acid (ABA) across a wide range of physiological processes (Depuydt & Hardtke, 2011). Stress conditions can further modulate this crosstalk, including reductions in GA biosynthesis via interactions with JA and ABA signalling pathways (Song et al., 2014; Weiss & Ori, 2007). These stress hormones have also been shown to have a positive effect on cannabinoid content in *C. sativa* via upregulating biosynthesis and increasing trichome density (Mansouri, Asrar, & Szopa, 2009; Welling et al., 2023).

GA biosynthesis begins with geranylgeranyl diphosphate (GGPP), which is predominantly derived from the plastidial MEP pathway (Kasahara et al., 2002). GGPP is cyclised by *ent*-copalyl diphosphate synthase (CPS) to *ent*-copalyl diphosphate (CPP), then converted to *ent*-kaurene by *ent*-kaurene synthase (KS) (Lemke et al., 2020). Oxidation by *ent*-kaurene oxidase (KO) and *ent*-kaurenoic acid oxidase (KAO) produces GA_{12} (Helliwell et al., 2001). Active GAs arise via branching steps catalysed by 2-oxoglutarate-dependent dioxygenases GA 3-oxidase (GA3ox), GA 13-oxidase (GA13ox), and GA 20-oxidase (GA20ox), with GA20ox representing the rate-limiting step (Hedden, 2020). GA homeostasis is tightly regulated transcriptionally and through deactivation by GA 2-oxidase (GA2ox) enzymes (Hedden, 2020).

Although biosynthesis is tissue-specific, long-distance GA transport is common, mediating systemic effects (Rizza & Jones, 2019). Signalling involves bioactive GA binding to the nuclear GA receptor GID1, inducing a conformational change that facilitates ubiquitin-mediated degradation of DELLA proteins (Yano et al., 2015). DELLAs, nuclear GRAS-family transcription regulators, are negative master regulators of GA signalling, repressing growth by inhibiting DNA binding of diverse transcription factors. Their degradation removes this repression, promoting growth. Through extensive protein interactions, DELLAs integrate GA with other

hormonal and developmental pathways, positioning them as central regulators in plant growth and stress responses (Davière & Achard, 2016).

HHISD varieties of the Green Revolution modulated GA signalling in several ways. Multiple HHISD rice varieties were developed independently but always involved deactivation of GA20ox, reducing endogenous GA (Hedden, 2003). Of the two rice genes encoding GA20ox, *OsGA20ox2* (sd1) was the breeding target, as disruption of *OsGA20ox1* caused severe developmental defects (Sasaki et al., 2002). In wheat, HHISDs arose from reduced height (*Rht*) mutations producing GA-insensitive varieties. *Rht* encodes a GRAS protein with a signalling-domain mutation that prevents GA-induced degradation, blocking downstream responses (Peng et al., 1999). Although not exploited during the Green Revolution, upregulating GA2ox enzymes offers an alternative strategy, inactivating GA and lowering its levels in crops (Hedden & Sponsel, 2015).

While genetic approaches are the most scalable means of manipulating GA levels, chemical treatments can induce transient GA-related phenotypes (Xiang et al., 2017). Gibberellic acid (GA_3), though a minor endogenous GA, is widely available and more potent than the abundant GA_1 and GA_4 (Hedden & Sponsel, 2015). High GA_3 concentrations can trigger sex reversal in *C. sativa*, inducing male flowers on genetically female plants (Galoch, 1978). Conversely, the triazole-type growth regulator Paclobutrazol (PBZ) reduces GA availability by reducing biosynthesis through *ent*-kaurene oxidase (KO) inhibition (Desta & Amare, 2021), simultaneously increasing chlorophyll and abscisic acid levels. PBZ has been applied across crops to enhance yield, stress resistance, and reduce plant height (Orozco-Meléndez et al., 2022). Both compounds are potent GA modulators, enabling the manipulation of GA-related traits and the identification of candidate gene targets (Khurshid et al., 1997; Spitzer & Bílovský, 2017; Sun et al., 2021; Xiang et al., 2017). In *C. sativa*, PBZ has been found in commercial fertigation additives to increase yield (Stone, 2014), while GA_3 can reduce flower biomass and cannabinoid content (Mansouri, Asrar, & Mehrabani, 2009), though mechanistic studies remain limited to hormone pathway expression (Oultram et al., 2024).

Here, we explored a HI focused Green Revolution-style approach in *C. sativa* by applying foliar GA_3 and PBZ to female clones at flowering onset. Using a multi-omics framework, including targeted cannabinoid and terpenoid quantification, SWATH MS/MS proteomics, and comparative RNA-sequencing, we assessed physiological and metabolic responses. Particular attention was given to PBZ's reported upregulation of defence pathways and secondary metabolism, providing insights into potential source–sink trade-offs influencing cannabinoid accumulation and highlighting GA-related breeding targets for crop improvement.

Results

Manipulation of the gibberellin pathway greatly affects C. sativa phenotype and harvest index

GA_3 and PBZ applications substantially altered the phenotypes of treated female IPK_CAN_57 clones (Figure 1) (Supplementary Tables S3 and S4). GA_3-treated plants were, on average 31.2% taller than Control plants, whereas PBZ were 66.8% shorter (p<0.001) (Figure 2). This corresponded to PBZ treatment also resulting in shorter branches (p<0.001) and fewer nodes (p<0.001), whereas there was no significant difference in the stem diameter between any of the groups (p=0.15).

Treatments caused significant alterations in resource allocation, with PBZ-treated plants having a mean harvest index of 53.5%, Control 31.3% and GA_3-treated 10.7% (p<0.001), despite total biomass not changing

significantly (p=0.92). This coincided with a higher mean total fresh flower weight in PBZ-treated plants of 58.3g, to the 11.3g of the GA_3-treated plants, although neither was significantly different to the Control of 34.6g (p=0.78 and p=0.84 respectively) (Figure 2). No difference in the size of individual flowers was observed (p=0.97) (Supplementary Figure S1), indicating the differences in flower weight were due to the increase in number of flowers produced per plant (Figure 2).

Inhibition of the gibberellin pathway increases cannabinoid accumulation but not terpenoid.

In addition to the significant phenotypic changes, manipulation of the gibberellin pathway instigated significant changes in the accumulation of secondary metabolites (Figure 3) (Supplementary Table S5). PBZ treatment significantly increased the concentrations of all cannabinoids measured except for CBGA (p=0.10), whereas GA_3 treatment did not significantly alter cannabinoid content (Figure 3A). This resulted in the mean concentration of total cannabinoids in PBZ-treated plants to be 84.9mg g^{-1}, whereas Control and GA_3-treated where 47.5mg g^{-1} and 40.9mg g^{-1}, respectively, correlating to a 78.6% increase in concentration for PBZ flowers compared to Control (p<0.001). No statistical difference in cannabinoid content was found between GA_3-treated and Control (p=0.55). Conversely, total terpenoid accumulation was not significantly affected by either treatment (p=0.35) (Figure 3B). The increase in cannabinoid content in PBZ-treated plants coincided with a 5.1% increase in trichome head size (Figure 2), compared to Control (p=0.04), while no difference was observed between Control and GA_3-treated trichomes (p=0.73) (Supplementary Table S6). The harvested and dried flowers of PBZ-treated plants contained 0.25ppm PBZ as a residue (Supplementary Figure S2).

Proteome quantification indicates the greatest differences mid-way through flowering.

The proteomes from flower tissue quantifying 2075 unique proteins of the three treatment groups were compared in triplicate (n=3) at 7, 21 and 35 into the flowering photoperiod using a principle component analysis to better quantify the impact of the treatments across the whole six-week flowering period (Figure 4A-C). Early in flowering (day 7) PC1 separated all treatments, although the PBZ and control groups showed some similarities in PC2 (Figure 4A). At mid-flowing stage (day 21) the greatest difference in proteomes was observed, with Control and GA3 separated by PC1, and Control and PBZ separated by PC2 (Figure 4B). Late in the flowering period (day 35), the proteomes of both GA_3 (GA3) and PBZ treatment groups shared similarities, while Control was separate (Figure 4C). As such, differences in the proteome on day 21 of flowering were considered more likely drivers of the observed phenotypic alterations between treatments. A $\log_2$fold change$\geq$ 1 cut-off, and an adjusted p value of 0.01 used to define differentially abundant proteins (DAP), yielding 311 DAPs in PBZ v Control, 301 in GA3 v Control and 390 in PBZ v GA3 on day 21 (Supplementary Table S7). DAPs at multiple time points were then identified (Supplementary Figure S2A).

The proteomes at day 21 indicated changes in primary metabolism with downregulation of key proteins in the glycolysis and citric acid cycles in GA_3-treated plants and up-regulation in PBZ-treated plants. Additionally, PBZ plants showed increased lipoxygenase (LOX) abundance which is associated with the breakdown of long-chain fatty acids (Supplementary Table S8).

Effect of GA pathway modulation on gene expression in floral tissue.

Single-end reads were generated from biological quadruplicates (n=4) 21 days into flowering, resulting in 361 million clean reads, 92.2% of which were mapped to the CBDRx reference genome with an average of 30.1 million reads per sample (Grassa et al., 2021) (Supplementary Table S9).

Differential gene expression analysis

The hierarchical clustering of RNA-seq data further supported proteomic PCAs (Figure 4D-E), with the samples from Day 7 of flowering showing mixed clustering of treatments (Figure 4D), whereas with samples from Day 21 (Figure 4E), each treatment grouped separately. Again, this indicates that this mid-flowering timepoint was key, and the majority of further analysis was focused on Day 21. Differential gene expression analysis was then performed with pairwise comparisons of each treatment, a $\log_2$fold change$\geq$ 1 cut-off, and an adjusted *p* value of 0.01 used to define differentially expressed genes (DEG), yielding 612 DEGs in PBZ v Control, 1993 in GA3 v Control and 1435 in PBZ v GA3 (Supplementary Table S10). DEGs in both time points were compared further to identify key genes (Supplementary Figure S3B).

Arabidopsis Gene Identifiers (AGIs) were assigned to DEG transcripts for gene ontology (GO) enrichment analysis (Supplementary Table S11). Many of the most significantly enriched biological process gene ontology terms involving the GA3 group were associated with photosynthesis and primary metabolism (GO:0015979, GO:0019684, GO:0006091, GO:0015977), whereas the Control vs PBZ comparison had more enriched terms associated with cell wall development and hormone signalling (GO:0010410, GO:0010383, GO:0009694, GO:0009739) (Supplementary Figure S4). All three comparisons shared enriched terms associated with the oxylipin pathway and sugar transport (GO:0006631, GO:0031408, GO:0005985). KEGG mapping (Supplementary Figure S5), additionally showed changes to photosynthetic and carbon fixation pathways (csav00195, csav00710) for GA3 plants and the fatty acid pathway (csav00591) for PBZ plants.

DEGs within pathways of interest were analysed to isolate the key drivers of the change in phenotypes of the experimental groups. These included changes in energy flow (source/sink dynamics, photosynthesis, and primary metabolism), hormone signalling (gibberellin, jasmonate, and abscisic acid), and secondary metabolite biosynthesis (fatty acid, MEP, hexanoate, and cannabinoid) (Figure 5, Supplementary Table S12).

Weighted gene co-expression network analysis (WGCNA)

WGCNA was used to further understand GA pathway manipulation on cannabinoid biosynthesis and phenotypic traits. Weighted co-expression network construction identified 40 modules (Supplementary Figure S6). To identify modules with strong associations with traits of interest module eigengenes were correlated with cannabinoid content (mg/g) (Figure 6A), and agronomic traits (Figure 6B). Eigengenes from the dark olive green module strongly correlated with all measured cannabinoids (r = 0.82 – 0.87, $p<0.01$) except CBGA (r = 0.43). In contrast, eigengenes from the magenta module showed strong correlations to both harvest index (r = 0.81, $p<0.01$) and flower weight (r = 0.67, $p<0.01$), and strong negative correlations with height (r = -0.74, $p<0.01$) and node number (r = -0.74, $p<0.01$). Genes that show a high degree of within-module connectivity are considered to have greater biological importance (Pei et al., 2017). Network plots show the top 20 most connected genes in the dark olive green (Figure 6C) and magenta (Figure 6D) modules (Supplementary Table S13). Five of the top seven hub genes in the dark olive green module highly correlated with cannabinoid content

code for cellulose synthases, and a gene that encodes in LOX11 of the oxylipin pathway was also in the top 15 most connected genes within this module (Figure 6C). In contrast, the top hub genes in the magenta module, highly correlated with harvest index, a measure of source/sink dynamics, are sucrose synthases, which catalyse the breakdown of sucrose into fructose and glucose (Figure 6D). Additionally, individual transcript trait correlations were performed (Supplementary Table S14), and transcript module membership summarised (Supplementary Table S15)

Comparison of proteomic and transcriptomic datasets.

The PCA of the proteomes and hierarchical clustering of the transcriptomes both showed the greatest differences in treatments mid-way through flowering (Figures 4B and 4E), highlighting the congruence of the two different -omics datasets. Additionally, this mid-flowering timepoint has been linked to the phase of active secretion of secondary metabolites into trichomes' storage cavities (Nolan, et al., 2025), which is therefore, key to understanding differences in cannabinoid productivity. Day 21 also resulted in a greater number of DEGs than day 7 in all comparisons (Supplementary Figure S3B).

Pathway enrichment analysis was performed on the AGIs of reciprocal best-hit BLASTs of differentially abundant proteins (DAPs). Allowing for the comparison with the transcriptomic-derived enrichments, and many of the most enriched GO terms and KEGG pathways in each possible comparison were shared across datasets (Supplementary Figures S4 and S5). A correlation of protein normalised area and transcript normalised counts was then performed on matches between the proteomic and transcriptomic datasets with a positive relationship in all treatment groups (Supplementary Figure S7). This strongly grounded both datasets and supported the biological significance of the shared terms (Supplementary Figures S4 and S5), given proteomic and transcriptomic datasets can have little to no correlation due to post-transcriptional, post-translational and protein degradation regulation (Haider & Pal, 2013; Maier et al., 2009; Vogel & Marcotte, 2012a). Thus, the correlation yet, independence of both transcriptomics and proteomics effectively validates both techniques (X. Wang et al., 2014). Further fine-scale analysis and interpretation focused on the transcriptome due to the greater resolution.

Identification of gibberellin oxidase genes.

Due to their importance in gibberellin biosynthesis and impact on Green Revolution breeding practices, a genome-wide identification of gibberellin oxidase (GAox) proteins was undertaken. To confirm and identify all *C. sativa* GAox genes, a BLASTP (E-value of e^{-10}) search using known *Arabidopsis thaliana* and *Oryza sativa* (rice) GAox proteins (Han & Zhu, 2011; Zhang et al., 2022). This analysis was complemented by screening for conserved domain profiles including 2OG-FeII_Oxy (PF03171) and DIOX_N (PF14226), as described by (Zhang et al., 2022). A total of 28 *C. sativa* GAox genes were identified and catalogued (Supplementary Table S16). To understand evolutionary relationships among these proteins, a phylogenetic tree was constructed using 61 GAox protein sequences from *C. sativa*, Rice and Arabidopsis (Figure 7). The *C. sativa* GAox proteins clustered with their counterparts from Arabidopsis and rice within distinct subfamilies, showing conserved motif characteristics of GAox proteins (Supplementary Figure S8). Additionally, treatment with GA_3 and PBZ significantly altered the expression of many of the identified GAox genes in this study (Figure 6). These expression changes aligned with observed variations in HI and cannabinoid accumulation (Figures 2 and 3), highlighting a potential regulatory role of GAox in these traits.

Discussion

GA pathways influence the yield of major C. sativa products.

Despite demonstrated efficacy in other crops and potential value for HHISD, GA modulation remains underexplored in *C. sativa* (Small, 2018). We assessed the effects of GA_3 and the biosynthesis inhibitor PBZ using morphological, chemotype, proteomic, and transcriptomic analyses, building on prior studies of GA-induced phenotypic responses (Garcia-de Heer et al., 2026; Hahm et al., 2023; Mansouri, Asrar, & Mehrabani, 2009; Oultram et al., 2024).

Modern agronomic practices favour high-density planting, making tolerance to crowding a key trait (Tang et al., 2018). GA inhibition decreases both height and branching in *C. sativa* (Figure 2), enabling higher planting density. Shorter plants also reduce lodging and facilitate integration with existing agricultural machinery, such as combine harvesters for semi-dwarf grains or automation in multi-level hydroponic systems. PBZ-treated plants produced more flowers (Figure 2), potentially enhancing seed yield when pollination occurs, consistent with previous reports in *in vitro*-grown *C. sativa* supplemented with PBZ (Ajdanian et al., 2024). Conversely, GA_3 induced taller plants while reducing the harvest index, which may benefit fibre production by yielding longer fibres and finer yarns (Westerhuis et al., 2019). GA inhibition also increased cannabinoid content, with clear applications in medical and recreational contexts (Figure 3). However, it needs to be noted that this study was conducted using a single high-CBD landrace, and the magnitude of phenotypic and chemotypic responses to GA_3 and PBZ treatments may differ compared to modern drug-type and industrial cultivars due to breeding selection, which could have affecting the GA pathway either directly or indirectly (Ren et al., 2021).

The diverse end uses of *C. sativa* complicate variety development, as reproductive (flower and seed) and vegetative (fibre and hurd) tissues produce distinct products. Breeding strategies that influence traits across multiple product types are therefore advantageous. This study indicates GA modulation provides a versatile tool for tailoring *C. sativa* morphology and chemistry for diverse agronomic and industrial objectives. However, further validation in seed and fibre contexts is needed. Additionally, PBZ residues in flowers exceed Food Standards Australia and New Zealand limits (0.01 ppm) (Food Standards Australia New Zealand, 2024) (Supplementary Figure S2), limiting its use to research, although alternative inhibitors, withholding periods or genetic approaches may be more suitable for production.

Modulation of GA pathway affects green revolution genes in C. sativa.

GA signalling and biosynthesis are tightly regulated to maintain homeostasis within the plant (Hedden, 2020), with GA_3 and PBZ treatments having been shown to increase and decrease internal GA concentrations respectively in wheat and rice (Nagar et al., 2021; H. Wu et al., 2019). Accordingly, GA_3 treatment was expected to suppress biosynthesis and perception while enhancing metabolism, with PBZ producing the opposite effect. These patterns, previously reported in rice and apple (Fan et al., 2018; Xiang et al., 2017) were largely confirmed in this study (Figure 5). An exception was a *GA2ox* gene (LOC115710658) that increased in PBZ-treated plants (Figure 5), contrary to expectations. This may reflect an annotation error in the CBDrX genome, although phylogenetic and motif analyses still group it with GA2ox enzymes (Figure 7, Supplementary Figure S8), warranting further validation.

Early GA biosynthesis enzyme genes *KS* (LOC115712980) and *KAO* (LOC115710887) were significantly responsive to GA and PBZ treatment (Figure 6), but knockouts of these genes induce extreme dwarfism and sterility, limiting their breeding utility (Hedden, 2003). Downstream, *GA20ox* genes, particularly *GA20ox2*, have been central to achieving high harvest index in rice, while *GA20ox1* primarily influences floral development and grain filling (Hedden, 2003). In *C. sativa*, *GA20ox1* (LOC115712114) and *GA20ox2* (LOC115715725) were differentially expressed between treatments (Figure 5) and strongly negatively correlated with HI (r = -0.77 and -0.92, Supplementary Table S14), with *GA3ox* (LOC115705300) showing a weaker correlation (r = -0.60). *GA20ox2* exhibited larger expression shifts, stronger trait correlations, and consistent differential expression at both day 7 and 21 of flowering (Supplementary Figure S3), consistent with previous work in rice (Cheng et al., 2022), potentially identifying it as the most promising target for GA pathway modulation in *C. sativa*.

GA catabolic enzymes influence GA signalling (Rieu et al., 2008). Expression of one of these enzymes, *GA2ox*, increased after GA_3 treatment (Figure 5), consistent with observations in *Phaseolus coccineus* (Thomas et al., 1999). In rice and Poplar hybrids, *GA2ox* upregulation or overexpression reduces height and internode length (Busov et al., 2003; Chu et al., 2019). However, in *C. sativa*, stable transgenic protocols remain challenging, making such an approach less feasible (Mohammad et al., 2024)..

Determining the applicability of a wheat-type *Rht* focussed GA modulation in *C. sativa* is less clear from this study. The approach has proven effective in other cereal crops because those species have a single *Rht*/GAI-type protein (whereas Arabidopsis has multiple), while to our knowledge, the number in *C. sativa* has yet to be determined (Hedden, 2003). DELLA proteins were absent from the SWATH proteomic library, and no DELLA-encoding genes were differentially expressed (Supplementary Table S10). GA_3 treatment reduced expression of the GA receptor homologue *GID1*, associated with DELLA degradation (Figure 5), suggesting that altering receptor expression and DELLA degradation could provide an alternative route for GA modulation in *C. sativa* (Dill et al., 2001).

GAox genes have been identified in various species, but their identity in *C. sativa* was incomplete. We identified 28 proteins (Supplementary Table S16), compared with 20 in *Zea mays* (Zhang et al., 2022), 38 in *Solanum tuberosum* (Chauhan et al., 2023), and 24 in *Vitis vinifera* (He et al., 2019). All 28 proteins clustered with Rice and Arabidopsis reference proteins (Figure 7) and showed conserved motifs (Supplementary Figure S8). Fifteen were found expressed in developing female flowers and responsive to GA_3 and/or PBZ treatment (Figure 5), supporting their identification and providing a foundation for their continued study in *C. sativa*.

Gibberellins alter source/sink dynamics, a key driver of changes to harvest index and floral yield in C. sativa.
HI has driven some of the largest yield gains in modern agriculture, valued for its stability across environments and genotypes (Unkovich et al., 2010). As an integrative trait, HI represents the efficiency of photosynthate allocation from generation in source tissues (leaves), transport (through the phloem), to sinks (flowers, seeds, roots, and trichomes) (Smith et al., 2018). Photo-assimilate unloading in sink tissue, not source production or transport, is the rate-limiting step (Patrick & Slewinski, 2013), and unloading restrictions can suppress photosynthesis itself (White et al., 2016). Accordingly, our transcriptomic and proteomic analyses focused on

floral sink tissue. The marked PBZ-induced HI increase (Figure 2) thereby reflects amplified sink strength, enhancing sugar utilisation and yield potential.

Sink strength integrates sink size and activity (Smith et al., 2018), with GA_3 treatment decreasing flower yield and PBZ treatment increasing it (Figure 2), reflecting changes to sink size. Sink activity depends on phloem unloading, largely mediated by *sucrose synthases (SUS)*, *SWEET* transporters, and hexose symporters (Osorio et al., 2014). Two *SUS* transcripts (LOC115705430, LOC115705483) were magenta module hub genes highly correlated with HI (Figures 6B, 6D) and upregulated in PBZ plants (Figure 5), coinciding with reduced *SUS2* protein (A0A7J6F7C7) in GA3 plants and increased galactosyltransferase (A0A803QB26) in PBZ plants (Supplementary Table S8). Several sugar transporters and *SWEET* homologues (LOC115716757, LOC115710321, LOC115722728, LOC115707412) were downregulated in GA3 plants or upregulated in PBZ plants (Figure 6). Overexpression of *SUS* in tomato increases fruit yield (Micallef et al., 1995), while *SWEET11/12* knockouts in Arabidopsis reduce sugar export and photosynthesis (L. Chen et al., 2012), supporting PBZ-induced enhancement of sink activity.

SNF-related kinases (SnRKs) regulate plant energy balance, downregulating energy-consuming processes under stress to redirect resources to tolerance (Crepin & Rolland, 2019). In this study, *SnRK* transcripts were upregulated in PBZ plants (LOC115722026, LOC115697460, LOC115707923) and downregulated in GA3 plants (LOC115711284, LOC115711285, LOC115725032), mirroring *SUS* expression patterns (Figure 5). Coordinated *SnRK* and *SUS* expression has been linked to enhanced sugar accumulation in Prunus persica fruit (W. Yu et al., 2021). In *C. sativa* flowers, this likely increased sucrose concentration, boosting floral biomass and energy availability for secondary metabolite biosynthesis. *SnRK* proteins have also been suggested to facilitate sugar transfer from flowers into trichomes (Conneely et al., 2021). As metabolically active, non-photosynthetic organs, trichomes act as a sink within the floral sink, with secondary metabolites serving as a final storage site for photosynthates.

Enhanced sink strength is also marked by increased respiratory metabolism and sugar catabolism (Fernie et al., 2004). PBZ-treated plants upregulated *pyruvate decarboxylase (PDC)* (LOC115718871, LOC115697036) and *phosphoenolpyruvate carboxylase (PEPC)* (LOC115704970, LOC115704928, LOC115704930) (Figure 5), boosting glycolysis and TCA activity. As the TCA cycle drives ATP synthesis (Zhang & Fernie, 2023), PBZ increases floral sink capacity and shifts HI toward flowers. Contrastingly, GA_3 treatment elevated *citrate synthase (CS)* expression (Figure 5), which can redirect photosynthates, with its downregulation enhancing secondary metabolite production in Arabidopsis (Fatland et al., 2005).

Pathway enrichment revealed photosynthesis and carbon fixation terms enriched in GA_3-treated plants versus Control and PBZ-treated (Supplementary Figures S4, S5), aligning with GA_3 application causing lighter leaves and PBZ application darker leaves (Figure 1). PBZ increases chlorophyll in *C. sativa* plantlets (Ajdanian et al., 2024), suggesting enhanced source strength. In GA3 flowers, chlorophyll-binding proteins (LOC115725330, LOC115696956, LOC115720381) were upregulated (Figure 6), indicating a compensatory increase in floral photosynthesis due to reduced sugar import. As floral tissue contributes little to total photosynthates (Osorio et al., 2014), this response mirrors GA_3 induced leaf chlorophyll reduction previously reported in C. sativa (Mansouri, Asrar, & Mehrabani, 2009).

Overall, GA modulation strongly influenced source/sink dynamics in *C. sativa*, and these shifts were likely the primary driver of the observed changes in HI in GA_3 and PBZ-treated plants. Key components of these dynamics include *SUS* enzymes, *SWEET* transporters, and *SnRK* proteins, which appear to act as major downstream targets of GA signalling. Their coordinated regulation enhances sink strength and carbohydrate allocation to flowers and trichomes, identifying them as promising molecular targets for HI-focused breeding in *C. sativa*.

The antagonistic relationship of GA with JA, ABA potentially influences phenotype and cannabinoid content.

Like the PBZ treatment used in this study, exogenous JA and ABA application have been previously shown to enhance cannabinoid content in *C. sativa* (Mansouri, Asrar, & Szopa, 2009; Welling et al., 2023), potentially through indirect mechanisms outside the cannabinoid biosynthetic pathway (Dimopoulos et al., 2025). GA is known to interact antagonistically with JA and ABA in multiple contexts (Song et al., 2014; Weiss & Ori, 2007). For instance, GA_3 treatment was found to reduce endogenous ABA content in *Rhynchostylis gigantea* (Phengphachanh et al., 2012), while PBZ treatment increased endogenous JA or ABA in *Ipomoea batatas*, *Mangifera indica* and *Malus prunifolia* (Opio et al., 2020; Si et al., 2023; Upreti et al., 2013). The idea that alterations in ABA and JA signalling contributed to the altered phenotypes caused by GA_3 and PBZ treatments in this study is consistent with the observed enrichment of JA and ABA signalling GO terms (Supplementary Figure S4). Transcriptomic analysis revealed reduced expression of *ABA insensitive 2* (LOC115702924) in PBZ treated plants (Figure 5), which is a negative regulator of ABA signalling linked to fatty acid biosynthesis (M. Chen et al., 2012), suggesting increased ABA sensitivity. The ABA receptor *pyrabactin resistance 1-like 4* (*PYL4*) (LOC115698161) was upregulated and identified as a hub gene in the magenta module (Figure 6B). PYL receptors activate *SnRK2*-mediated ABA signalling, which has been associated with enhanced stress responses and altered secondary metabolism (Crepin & Rolland, 2019; Pri-Tal et al., 2024).

LOX enzymes of the fatty acid pathway, precursors for both JA and cannabinoids, were upregulated in PBZ and GA_3-treated plants compared to Control (LOC115709296, LOC115722276, LOC115722275, LOC115719614, LOC115720530), although generally more strongly in PBZ treated plants (Figure 5). Downstream JA biosynthetic enzymes *AOC3* (LOC115699327) and *OPR2* (LOC115706393) were also upregulated in PBZ plants, suggesting increased JA biosynthetic activity (Figure 5). In contrast, the JA signalling repressor *jasmonate-zim domain 9 JAZ9* (LOC115714189) was upregulated in GA_3-treated plants (Figure 5); JAZ proteins are degraded when bioactive JA-Ile binds, lifting gene repression (Pauwels & Goossens, 2011). *Jasmonate resistance 1 (JAR1)* (LOC115705838), mediating JA-Ile conjugation, was additionally differentially expressed across both time points (Supplementary Figure S3, Table S6).

Additionally, the effect of JA and ABA on secondary metabolite biosynthesis can be synergistically improved by sucrose (Loreti et al., 2008), whereas high tissue glucose levels inhibit GA biosynthesis (Gibson, 2004). Moreover, GA-ABA interactions are known to modulate sugar transport in *Vitis vinifera* (Murcia et al., 2018). Thus, the potential alterations of floral sucrose levels instigated by GA modulation could compound the positive effect of increased JA and ABA signalling on cannabinoid levels and underscore their potential roles in PBZ-induced phenotypes.

It is important to keep in mind that changes in transcript or protein abundance within a hormone pathway do not necessarily correspond to predictable changes in hormone pool levels, as transcriptomic, proteomic, and metabolomic outputs are often non-linearly coupled (Symons et al., 2008; Vogel & Marcotte, 2012b). As hormone levels were not determined in the present study, the effects of the treatments on endogenous GA, JA and ABA levels are therefore uncertain. However, this does not preclude inference of hormonal interactions, also given that plant hormone responses are not solely determined by hormone abundance, as altered sensitivity or downstream signalling can induce substantial phenotypic and physiological changes without major changes in the underlying hormone pool (Weijers & Wagner, 2016). Taken together, the transcriptional patterns observed in this study suggest that the altered cannabinoid accumulation and phenotypes in GA_3 and PBZ-treated plants reflects interactions between GA, JA, and ABA signalling pathways.

Primary metabolism and fatty acid pathway (not terminal synthases) specify cannabinoid accumulation.

GA modulation strongly altered cannabinoid content in PBZ-treated plants but left terpenoid levels unchanged (Figure 3). This is consistent with the effects of GA3 application on *C. sativa* in previous studies (Mansouri, Asrar, & Mehrabani, 2009; Oultram et al., 2024). Although, Hahm *et. al.* (2023) found that the GA inhibitor diniconazole did not affect cannabinoid levels, potentially due to differences in treatment, genotype, or mechanisms between diniconazole and PBZ.

Despite both pathways drawing from GPP in the MEP pathway (Apicella et al., 2022), cannabinoid accumulation appears regulated independently of the MEP pathway. Although *4-hydroxy-3-methylbut-2-enyl diphosphate synthase (HDS)* (LOC115720893), the MEP pathway's rate-limiting enzyme (Yeo et al., 2022), was upregulated in GA_3-treated plants (Figure 5), this did not elevate cannabinoids or terpenoids (Figure 3), reinforcing that alternative regulatory mechanisms drive secondary metabolite accumulation outside the specific terpenoid biosynthetic pathways.

Both GA_3 and PBZ treatments induced widespread changes in gene expression associated with the cannabinoid pathway (Figure 6), yet these changes did not consistently correlate with final cannabinoid concentrations (Figure 3). In GA_3-treated plants, cannabidiolic acid synthase (CBDAS) gene expression (LOC115697762) and protein abundance (A0A0E3TIL8, Supplementary Table S8) increased, consistent with previous studies suggesting that increases in terminal synthase abundance are not critical for cannabinoid accumulation (Apicella et al., 2022; Yeo et al., 2022). Multiple *aromatic prenyltransferase (APT)* genes also showed increased expression in GA_3-treated plants (Figure 6), catalysing the formation of CBGA, a theorised as rate-limiting step (Sands et al., 2023), yet this did not alter CBGA or total cannabinoid content (Figure 3). Similarly, *polyketide synthase (PKS)* (LOC115699293, LOC115700696) and *olivetolic acid cyclase (OAC)* (LOC115723434, LOC115723437) transcripts were upregulated in GA_3-treated plants (Figure 5) without increasing cannabinoids (Figure 3). In contrast, upstream hexanoate pathway enzymes genes *acyl-activating enzyme (AAE)* (LOC115695955) and *aldehyde dehydrogenase (ALDH)* (LOC115721408) were upregulated in PBZ-treated plants, coinciding with increased cannabinoid content (Figure 5). *AAE* is notable for its high expression in trichomes (Stout et al., 2012), consistent with increased primary metabolism during peak cannabinoid biosynthesis in *C. sativa* trichomes (Nolan, Guo, Liu, et al., 2025).

PBZ-treated plants had increased abundance of acetyl-CoA carboxylase proteins (A0A803PTH1 and A0A803QYK8, Supplementary Table S8), which carboxylate acetyl-CoA to form malonyl-CoA, required for condensation with hexanoyl-CoA to produce olivetol, the cannabinoid precursor in the hexanoate pathway (Yeo et al., 2022), and is the rate-limiting step of fatty acid biosynthesis (Y. Wang et al., 2022). Acetyl-CoA C-acetyltransferase (ACAT) (A0A7J6DSS6) also increased across all time points in PBZ-treated plants (Supplementary Table S8), enabling β-oxidation of long-chain fatty acids to saturated C18 fatty acids (Hiremath et al., 2006). These saturated fatty acids are converted to linoleic acid C18:2, the LOX pathway precursor, by fatty acid desaturase FAD2 (Dar et al., 2017). Welling et al. (2023) suggested increased desaturase expression drives cannabinoid increases following methyl-jasmonate treatment, consistent with the decreased *FAD2* expression in GA_3 and increased expression in PBZ-treated plants observed here (Figure 5). LOX proteins also increased in PBZ-treated plants (Supplementary Table S8), and *csLOX11* (LOC115723988) was a hub gene in the cannabinoid-correlated dark olive-green module (Figure 7A). LOX catalyses one step of the breakdown of unsaturated C18 fatty acids to hexanal, increasing hexanoate precursor availability (Stout et al., 2012). GA pathway modulation mirrored these trends, with every hexanoate step from hexanal to hexanoyl-CoA inhibited by GA_3 treatment or induced by PBZ treatment (Figure 6), supporting prior findings that hexanoic acid application elevates cannabinoid content (Birenboim et al., 2024).

These findings suggest that PBZ boosts cannabinoid content by enhancing long-chain fatty acid biosynthesis and degradation, driving hexanoyl-CoA production via the hexanoate pathway (Apicella et al., 2022). This supports Stout et al.'s (2012) hypothesis that this pathway is the primary route for cannabinoid precursor formation. In contrast, the broad upregulation of cannabinoid pathway genes in GA_3 plants supports previous findings that the cannabinoid-specific enzymes play a minor role in final cannabinoid accumulation compared with the availability of fundamental precursors.

Changes in cannabinoid accumulation alters trichome morphology, not initiation

GAs promote trichome development in Arabidopsis (Perazza et al., 1998), yet GA_3 application reduces cannabinoid accumulation in *C. sativa* (Mansouri, Asrar, & Mehrabani, 2009; Oultram et al., 2024). JA stimulates trichome initiation in multiple species (Li et al., 2021), including *C. sativa* and has been linked to increased cannabinoid content (Huang et al., 2024). Despite observed JA signalling changes (Figure 5), trichome initiation gene expression remained unchanged in this study (Supplementary Materials S12).

However, PBZ treatment resulted in slightly larger trichome heads (Figure 2), which correlated with increased cannabinoid content (Figure 3), and are a target in modern drug-type breeding (Nolan, et al., 2025; Small & Naraine, 2016). Although not seen here, GA_3 can reduce trichome size in *C. sativa* (Mansouri, Asrar, & Mehrabani, 2009; Oultram et al., 2024). Cellulose synthase-like proteins were hub genes in the dark olive-green module (Figure 7C) and altering cellulose synthase activity changes trichome phenotypes in Arabidopsis (Bischoff et al., 2010). Cannabinoids accumulate in subcuticular trichome cavities, which expand through extensive cell wall remodelling (Livingston et al., 2022; Tissier et al., 2017). Membrane-bound cellulose synthases may support this expansion, yet it remains unclear whether increased cavity capacity drives higher cannabinoid biosynthesis or results from it in PBZ-treated plants.

Conclusion

Using a multi-omics approach, we explored how GA pathway modulation shapes *C. sativa* phenotypes. GA_3 treatment promoted tall, low HI plants potentially suited to fibre and hurd production, whereas PBZ inhibition generated HHISD plants with enhanced cannabinoid content for cannabinoid production. *GA20ox* emerged as a key nexus for GA-related traits. Altered *SUS* and *SnRK* expression suggested shifts in sugar transport and source–sink dynamics associated with the observed phenotypic differences. In cannabinoid biosynthesis, hexanoyl-CoA availability, rather than downstream enzyme activity, appeared limiting, potentially linked to long-chain fatty acid metabolism, exemplified by increased *FAD2* expression and ACAT abundance in PBZ-treated plants. Collectively, these findings suggest that targeted manipulation of GA signalling may provide opportunities to develop *C. sativa* varieties suited to different end uses and offer a framework for future investigations into the relationships between hormone regulation, resource allocation, and cannabinoid biosynthesis.

Materials and Methods

Plant production and treatments to modify gibberellin pathway

All work involving plant cultivation and material maintenance was conducted under NSW Low-THC Industrial Hemp Licence No. 52204 and complied with all relevant legislative and regulatory requirements. *C. sativa* germplasm (IPK_CAN_57) was obtained from the Leibniz Institute of Plant Genetics and Crop Plant Research (Leibniz-Institut für Pflanzengenetik und Kulturpflanzenforschung (IPK), Germany), imported under a federal Office of Drug Control (ODC) license to import No. 1820928 and handled under the Food and Agriculture Organization of the United Nations governed Standard Material Transfer Agreement (sMTA).

Seeds from IPK_CAN_57, a dioecious, CBD-dominant (chemotype III; THC <1.0%) drug-type hemp landrace were germinated, and seedlings with 2–4 true leaves were sexed under a 12:12 photoperiod, before a single female was selected for revegetation as a mother plant.

On Day 1, cuttings were taken from this mother and rooted in propagation trays (EazyPlug) for 14 days under LED lights (18:6 photoperiod, 100–150 µmol m^{-2} s^{-1}, 26 °C). Eighteen clones were potted in a hydroponic mix (70% coco coir, 30% perlite, 2L pot) supplemented with Osmocote Pro-3-4M (4.3 g L^{-1}) and grown for 12 days under vegetative conditions (18:6 photoperiod, 300–500 µmol m^{-2} s^{-1}, 26 °C).

1M stock solutions of gibberellic acid (GA_3) (Austratec Pty Ltd, Melbourne, Australia) and paclobutrazol (PBZ) (Austratec Pty Ltd, Melbourne, Australia) were made in 0.1 M NaOH and ethanol respectively, before diluted to working concentrations immediately before application. On Day 26, clones were assigned to treatments (n=6) of 200ppm GA_3 (GA3), 50ppm PBZ (PBZ), or distilled water (Control) (Supplementary Table S1), and foliar sprayed with solutions containing 0.1% Tween-20 (Austratec) until thoroughly coated. Treatments were repeated on Day 28, coinciding with the transition to flowering conditions (12:12 photoperiod, 1000 µmol m^{-2} s^{-1}, 26 °C), and Day 30. After 42 days of flowering (Day 70), plants were harvested and agronomic traits recorded, including height, branch length, stem diameter, node count. Flowers were hand trimmed to calculate flower yield, and harvest index,

$$Harvest\ index\ (\%) = fresh\ flower\ weight(g) \div total\ above\ ground\ biomass\ (g)\ \times 100$$

Apical buds were dried in darkness at 15 °C and 10% relative humidity for two weeks for secondary metabolite analysis. Individual flowers were dissected for morphological measurements (n=60) (Supplementary Figure S1A), and intact trichome heads were isolated by agitating ~1 g of dried flower in an ice/water slurry for 2 min, filtered through 220, 125, and 25 µm sieves, and mounted on microscope slides for head diameter measurements (n=180) (Supplementary Figure S1B).

Tissue sampling for secondary metabolite analysis, Protein extraction and RNA isolation

Apical shoot buds were collected from each clone weekly starting from Day 0 of flowering (Day 28 of the experiment) to analyse phenotypic changes comprehensively using omics techniques. Samples for protein and RNA were flash-frozen and stored at -80°C until required. RNA was purified from 50mg samples from day 7 and 21 of flowering as per the manufacturer's instructions (Qiagen RNeasy Mini Kit) for downstream RNA sequencing.

Protein extraction

The following method was adapted from Niu et al., (2018).

50-100mg of apical flower tissue was ground, and 2ml extraction solution (1% SDS, 0.1 M tris-HCl (pH 6.8), 2 mM disodium ethylenediaminetetraacetate (NA_2-EDTA), 20 mM dithiothreitol (DTT) and 2mM phenylmethylsulfonyl fluoride (PMSF) added before centrifuging for 3 minutes (20 000 *g*). 750µL of the supernatant was removed, the protein was precipitated with cold 20% TCA/acetone (1:1) solution, incubated on ice for 5 minutes, and centrifuged again. After the supernatant was discarded, the precipitate was washed with 1ml 90% methanol and centrifuged again before this washing step was repeated. Protein was then dried for 1-2 minutes using an aspiration machine until visibly dry. Samples from days 7, 21 and 35 of flowering were used for proteome quantification.

Secondary metabolite analysis

The following method was adapted from Dimopoulos et al. (2024).

Chemicals and reagents

HPLC grade acetonitrile, methanol, ethanol and certified cannabinoid and terpenoid standards were purchased from Sigma-Aldrich (Merk Pty. Ltd.) and UltraPure RNase-Free distilled water from ThermoFisher Scientific. Standards were used to create calibration curves with seven concentrations between 3.9µg/mL and 250µg/mL (Supplementary Table S2).

Extraction procedure

Flower material (100mg) was pulverised in a mortar and pestle after being frozen in liquid nitrogen before extraction of secondary metabolites using ethanol containing the internal standard tridecane (1mL, 0.22% v/v). The solution was sonicated in a 30°C water bath for 30 minutes and left overnight at room temperature. Solutions were centrifuged at 15,000rpm for 10 minutes after being vortexed briefly. An aliquot was then transferred neat for terpene analysis and diluted 1:20 with ethanol for cannabinoid analysis.

GC-FID quantification of terpenes

An Agilent 6850 GC system fitted with a SGE BPX5 capillary column (50m length, 220µm ID, 1.00µm film thickness) was used to analyse terpenoids. Hydrogen was used as the carrier gas at a rate of 1.2mL/min. The

injected volume was 1µL. The inlet temperature was at 280°C. The split ratio was 5:1. The oven temperature was maintained at 50°C for 1 min, then raised to 300°C at 8°C/min, held at 300°C for 10mins. A Flame Ionisation Detector (FID) was used with the GC. The FID temperature was at 260°C, the hydrogen flow was 30.0mL/min and the air flow was 300.0mL/min. Raw data was processed using Agilent OpenLab software (Version 2.7).

HPLC-UV quantification of cannabinoids

Samples were analysed for cannabinoid content on an Agilent 1260 Infinity II HPLC system based on modified conditions of Hewavitharana et al. (2022). An Agilent Poroshell C18, 2.7 µm, 2.1x150mm column was used. The column temperature was held at 30 °C. The injection volume was 1µL. The chromatographic analysis was performed using mobile phases containing MilliQ water with 0.1% (v/v) formic acid (mobile phase A), acetonitrile (mobile phase B), methanol (mobile phase C). The flow rate was 0.3 mL/min. A gradient elution started with 35% A, 50% B, 15% C up to 0.5min, then gradually changed to 28% A, 60% B, 12% C at 6min, 14% A, 80% B and 6% C at 11 min, 1% A and 99% B at 12 min, held 1% A and 99% B until 12.5 min. The mobile phase was then returned to the starting composition of 35% A, 50% B, 15% C over 0.5 min, and re-equilibrated for 5 min prior to the next injection. Raw data was processed using Agilent OpenLab software (Version 2.7) and used to quantify cannabichromenic acid (CBCA), cannabidiolic acid (CBDA), cannabidivarinic acid (CBDVA), cannabigerolic acid (CBGA) and tetrahydrocannabinolic acid (THCA).

Proteome Analysis

Adapted from Guo et al., (2022), the protein was quantified from triplicates of each treatment using floral samples (n=3) from day 7, 21 and 35 after flowering was induced using a SWATH MS/MS approach.

The samples were analysed using an Ekspert nano LC400 uHPLC (SCIEX, Canada) coupled with a TripleTOF 6600 quadrupole time-of-flight (QTOF) mass analyser (SCIEX, Canada) equipped with a PicoView nanoflow (New Objective, USA) ion source. A trap column (5mm × 300 mm, C18 3 mm, SGE, Australia) and an analytical column (75 mm × 150mm ChromXP C18 CL 3 mm, SCIEX, Canada) were utilised.

Peptide quantification was adapted from Dimopoulos et al., (2024) and used the same HPLC and mass spectrometry conditions as the information-dependent acquisition (IDA) mode, with slight modifications. Data acquisition was conducted using a SWATH approach, performing product ion MS/MS analysis across a m/z range of 350 to 1,500. The product ion window was set to 6 Da, and collision energy ranged from 16 to 60V. Spectral library generation was performed similarly to the original study. A total of 27 samples ((1 control +2 treatments) × 3 time points × 3 replicates) were searched collectively using the Paragon algorithm in ProteinPilot software (Version 5.0.2, SCIEX). The search utilised a *C. sativa* database from Uniprot (Downloaded Aug 2023), resulting in a final spectral library comprising 2281 distinct proteins with a critical false discovery rate of 1%. Spectral alignment and targeted data extraction of SWATH-MS data were performed using the SWATH Processing Micro App in PeakView (Version 1.2, SCIEX) with an extraction window of 25 minutes. Parameters included the selection of 15 peptides, 15 transitions, and a peptide confidence threshold of 95% with a critical false discovery rate of 1%. Additionally, shared peptides were excluded, and the extracted ion chromatogram width was set at 50 ppm.

RNA-seq, assembly and annotation

Quadruplicate samples (n=4) of each treatment group sampled at day 7 and 21 of flowering were sequenced through a paid service at the Australian Genome Research Facility (AGRF) using the Illumina NovaSeq 6000 single-end (100bp) flow cell. CLC Genomics Workbench 11.0.1. using default settings was used to map and process sample reads against the CBDrx reference genome (Grassa et al., 2021).

Statistical analysis and visualisations

All analysis was performed using R (version 4.2.1) (RStudio Team, 2020), Venn diagrams were created with Venny (v2.1) (Oliveros, 2015).

Agronomic and Secondary metabolite analysis

ANOVAs and Tukey's post hoc analysis were performed, and figures produced using the ggplot2 package (v3.5.0) (Wickham, 2016).

Proteomic analysis

The functional annotation of the identified *C. sativa* flower proteome was performed by aligning the protein sequences against the UniProtKB/SwissProt Arabidopsis database (updated as of October 2023) using BLASTP, with an e-value cut-off of 10^{-5}. Subsequently, the *Arabidopsis thaliana* genome accessions (AGIs) corresponding to the best-matching proteins were extracted for subsequent bioinformatic analyses. Differential analyses were conducted using a Student's t-test. Proteins exhibiting a *p*-value less than 0.05, along with an average fold change (FC) greater than 1.0 were designated as differentially abundant proteins (DAPs) in this study. The AGI identifiers of the identified DAPs were subjected to Kyoto Encyclopedia of Genes and Genomes (KEGG) pathways enrichment analysis using the ClusterProfiler package (v4.6.2) in R (Wu et al., 2021). Welch's t-test was used to determine the significance difference between treatments and Control, with outliers more than two standard deviations away from the mean removed.

Transcriptomic analysis

Total counts were exported and transcripts with counts below 10 excluded, before being normalised using a median of ratios method using the DESEQ2 package (v1.38.3) (Love et al., 2014). Differential expression analysis was performed on the three experimental groups to produce three pairwise comparisons. P-values were adjusted using the Benjami-Hochberg method. A $\log_2$ fold change≥1 and an adjusted p-value of 0.01 cut-off criteria were applied to identify differentially expressed genes (DEGs).

Raw reads were normalised using a variance stabilising transformation (Love et al., 2014). A power of 26 was chosen to ensure a scale-free topology model with a signed R^2 >0.85 and mean connectivity < 100. Before a signed, weighted correlation networks were produced using the WGCNA package (v1.73) (Langfelder & Horvath, 2008). The module eigengenes (MEs) is the first component of a PCA of each module and reflects the common expression patterns of all the genes in the module. MEs were calculated, and Pearson's correlation between MEs and traits of interest was used to probe relationships modules and traits.

KEGG and gene ontology (GO) pathway enrichment analysis was performed on DEGs using the clusterProfiler package (v4.6.2) (Wu et al., 2021), with the CBDrx genome (KEGG) and the genome-wide annotation package for Arabidopsis, org.At.tair.db (v3.16.0) to identify enriched biological processes, cellular components, and molecular functions (Carlson, 2019). Arabidopsis homologues with corresponding Arabidopsis Gene Identifiers

(AGI) were identified using mmseq2 reciprocal best hits of the protein sequences. Reciprocal best hits using BLASTn of the mRNA sequences were used where no protein sequence hits occurred.

Identification of gibberellin oxidase proteins

Protein sequences from *Oryza sativa* (17) (Zhang et al., 2022) and *Arabidopsis thaliana* (16) (Han & Zhu, 2011) were downloaded from the Uniprot database (https://www.uniprot.org, accessed on 22 December 2024) and used as reference sequences to query the *C. sativa* protein dataset which was obtained from the NCBI CS10 genome assembly a BLASTP search (E-value of e^{-10}) (Zhang et al., 2022) was conducted to identify candidate *C. sativa* gibberellin oxidase (GAox) sequences. Candidate sequences were then screen to ensure they contained conserved domain, specifically 2OG-FeII_Oxy [PF03171] and DIOX_N [PF14226] obtained from the Pfam database (database (http://pfam.xfam.org) resulting in 113 sequences. Multisequence alignments and phylogenetic analyses were performed using MEGA11: Molecular Evolutionary Genetic Analysis version 11.0.13 (Tamura et al., 2021) to confirm the identity of candidate GAox sequences, before unrooted phylogenetic trees were generated using the neighbor-joining construction method with 1000 bootstrap replicates to assess branch support. Sequences that did not cluster with known GAox groups from Arabidopsis and Rice were excluded, yielding 28 putative *C. sativa* GAox sequences. Phylogenetic tree visualization was performed using FigTree v1.4.3 (v3.62)(G. Yu et al., 2017). To further investigate conserved motifs, the 28 *C. sativa* sequences, along with the reference sequences from Arabidopsis and rice, were submitted to the MEME suite (v5.5.7) (https://meme-suite.org/meme/, accessed on 06 January 2025). The analysis was conducted with a maximum of 15 motifs specified and default setting applied. Refer to Supplementary Table S16 for putative GAox nomenclature and sequences, and Supplementary Table S17 for EC numbers of these and all other enzymes discussed throughout the manuscript.

Data availability

The RNA-Seq data underlying this article are available in the Sequence Read Archive (SRA) Database at https://www.ncbi.nlm.nih.gov/sra/PRJNA1195153, and can be accessed with PRJNA1195153. The raw mass spectrometry proteomic data used in this study is available in the Southern Cross University research portal (https://researchportal.scu.edu.au) and are available under DOI: 10.25918/data.443.

Funding

This work was supported by funding from the Australian Research Council (ARC) Linkage project [grant number LP210200606]. In addition, Lennard Garcia-de Heer received a stipend from Southern Cross University, and Xuan Chen was awarded a scholarship from China Scholarship Council.

Acknowledgements

The authors would like to acknowledge Andrew Kavasilas for enabling this work as industry partner of LP210200606 and for ensuring that it aligns with industry needs, and Quintin Meredith for performing the protein extractions.

Author Contributions

LG: Conceptualisation, Formal Analysis, Methodology, Investigation, Writing – Original Draft

MN: Investigation, Methodology, Formal analysis, Writing – Review and Editing

QG: Formal analysis, Data curation, Writing – Review and Editing

JM: Conceptualisation, Resources, Supervision, Writing – Review and Editing

ND: Investigation, Methodology, Writing – Review and Editing

LL: Investigation, Methodology, Writing – Review and Editing

XC: Conceptualisation, Methodology, Investigation, Supervision, Writing – Review and Editing

TK: Conceptualisation, Resources, Supervision, Funding acquisition, Project administration, Writing – Review and Editing

Disclosures

The authors declare that they have no known competing financial interests or personal relationships that could have appeared to influence the work reported in this paper.

References

Ajdanian, L., Arouiee, H., Jones, A. M. P., Hesami, M., Nemati, H., & Pepe, M. (2024). Investigating the impact of paclobutrazol and tannic acid on floral development of in vitro -grown cannabis plantlets. *Heliyon*, *10*(17), e36768. https://doi.org/10.1016/j.heliyon.2024.e36768

Andre, C. M., Hausman, J. F., & Guerriero, G. (2016). *Cannabis sativa*: The plant of the thousand and one molecules. *Frontiers in Plant Science*, *7*(19), 1–17. https://doi.org/10.3389/fpls.2016.00019

Apicella, P. V., Sands, L. B., Ma, Y., & Berkowitz, G. A. (2022). Delineating genetic regulation of cannabinoid biosynthesis during female flower development in *Cannabis sativa*. *Plant Direct*, *6*(6), 1–8. https://doi.org/10.1002/pld3.412

Birenboim, M., Chalupowicz, D., Kenigsbuch, D., & Shimshoni, J. A. (2024). Improved long-term preservation of Cannabis inflorescence by utilizing integrated pre-harvest hexanoic acid treatment and optimal post-harvest storage conditions. *Plants*, *13*(7). https://doi.org/10.3390/plants13070992

Busov, V. B., Meilan, R., Pearce, D. W., Ma, C., Rood, S. B., & Strauss, S. H. (2003). Activation tagging of a dominant gibberellin catabolism gene (GA 2-oxidase) from poplar that regulates tree stature. *Plant Physiology*, *132*(3), 1283–1291. https://doi.org/10.1104/pp.103.020354

Carlson, M. (2019). org.At.tair.db: Genome wide annotation for Arabidopsis. *R Package Version 3.8.2*.

Chauhan, H., Aiana, & Singh, K. (2023). Genome-wide identification of 2- oxoglutarate and Fe (II)-dependent dioxygenase family genes and their expression profiling under drought and salt stress in potato. *PeerJ*, *11*(Ii). https://doi.org/10.7717/peerj.16449

Chen, L., Qu, X., Hou, B., Sosso, D., Osorio, S., Fernie, A. R., & Frommer, W. B. (2012). Sucrose efflux mediated by SWEET proteins as a key step for phloem transport. *Science*, *335*(6065), 207–211. https://doi.org/https://doi.org/10.1126/science.1213351

Chen, M., Du, X., Zhu, Y., Wang, Z., Hua, S., Li, Z., Guo, W., Zhang, G., Peng, J., & Jiang, L. (2012). Seed Fatty Acid Reducer acts downstream of gibberellin signalling pathway to lower seed fatty acid storage in Arabidopsis. *Plant, Cell and Environment*, *35*(12), 2155–2169. https://doi.org/10.1111/j.1365-3040.2012.02546.x

Cheng, X., Huang, Y., Tan, Y., Tan, L., Yin, J., & Zou, G. (2022). Potentially useful dwarfing or semi-dwarfing genes in rice breeding in addition to the sd1 gene. *Rice*, *15*(1). https://doi.org/10.1186/s12284-022-00615-y

Chu, Y., Xu, N., Wu, Q., Yu, B., Li, X., Chen, R., & Huang, J. (2019). Rice transcription factor OsMADS57 regulates plant height by modulating gibberellin catabolism. *Rice*, *12*(1), 1–14. https://doi.org/10.1186/s12284-019-0298-6

Conneely, L. J., Mauleon, R., Mieog, J., Barkla, B. J., & Kretzschmar, T. (2021). Characterization of the *Cannabis sativa* glandular trichome proteome. *PLoS ONE*, *16*(4 April), 1–26. https://doi.org/10.1371/journal.pone.0242633

Crepin, N., & Rolland, F. (2019). SnRK1 activation, signaling, and networking for energy homeostasis. *Current Opinion in Plant Biology*, *51*, 29–36. https://doi.org/10.1016/j.pbi.2019.03.006

Davière, J. M., & Achard, P. (2016). A pivotal role of DELLAs in regulating multiple hormone signals. *Molecular Plant*, *9*(1), 10–20. https://doi.org/10.1016/j.molp.2015.09.011

Depuydt, S., & Hardtke, C. S. (2011). Hormone signalling crosstalk in plant growth regulation. *Current Biology*, *21*(9), R365–R373. https://doi.org/10.1016/j.cub.2011.03.013

Desta, B., & Amare, G. (2021). Paclobutrazol as a plant growth regulator. In *Chemical and Biological Technologies in Agriculture* (Vol. 8, Number 1). Springer Science and Business Media Deutschland GmbH. https://doi.org/10.1186/s40538-020-00199-z

Dill, A., Jung, H. S., & Sun, T. P. (2001). The DELLA motif is essential for gibberellin-induced degradation of RGA. *Proceedings of the National Academy of Sciences of the United States of America*, *98*(24), 14162–14167. https://doi.org/10.1073/pnas.251534098

Dimopoulos, N., Guo, Q., Liu, L., Azman, R., Garcia-de Heer, L., Nolan, M., Mieog, J. C., Barkla, B. J., & Kretzschmar, T. (2025). Regulation of secondary metabolism in *Cannabis sativa* glandular trichomes by abscisic acid and water deficit stress during late flowering development. *Plant Stress*, *15*. https://doi.org/10.1016/j.stress.2025.100799

Dimopoulos, N., Guo, Q., Purdy, S. J., Nolan, M., Halimi, R. A., Mieog, J. C., Barkla, B. J., & Kretzschmar, T. (2024). From dawn 'til dusk: daytime progression regulates primary and secondary metabolism in Cannabis glandular trichomes. *Journal of Experimental Botany*, erae148. https://doi.org/10.1093/jxb/erae148

Fan, S., Zhang, D., Gao, C., Wan, S., Lei, C., Wang, J., Zuo, X., Dong, F., Li, Y., Shah, K., & Han, M. (2018). Mediation of Flower Induction by Gibberellin and its Inhibitor Paclobutrazol : mRNA and miRNA Integration Comprises Complex Regulatory Cross-Talk in Apple. *Plant & Cell Physiology*, *59*(August), 2288–2307. https://doi.org/10.1093/pcp/pcy154

Fatland, B. L., Nikolau, B. J., & Wurtele, E. S. (2005). Reverse genetic characterization of cytosolic acetyl-CoA generation by ATP-citrate Lyase in Arabidopsis. *The Plant Cell*, *17*, 182–203.

Fernie, A. R., Carrari, F., & Sweetlove, L. J. (2004). Respiratory metabolism: Glycolysis, the TCA cycle and mitochondrial electron transport. *Current Opinion in Plant Biology*, *7*(3), 254–261. https://doi.org/10.1016/j.pbi.2004.03.007

Food Standards Australia New Zealand. (2024). *Schedule 20 - Maximum residue limits*. Australia New Zealand Food Standards Code. https://www.legislation.gov.au/F2024L01358/latest/text

Galoch, E. (1978). The hormonal control of sex differentiation in dioecious plants of hemp (*Cannabis sativa*): The influence of plant growth regulators on sex expression in male and female plants. In *Acta Societatis Botanicorum Poloniae* (Vol. 47, Numbers 1–2, pp. 153–162). https://doi.org/10.5586/asbp.1978.013

Garcia-de Heer, L., Kretzschmar, T., & Mieog, J. (2026). Harnessing Sex Reversion via Chemical Intervention in *Cannabis sativa* L. *Plants*, *15*(9). https://doi.org/10.3390/plants15091291

Garcia-de Heer, L., Mieog, J., Burn, A., & Kretzschmar, T. (2024). Why not XY? Male monoecious sexual phenotypes challenge the female monoecious paradigm in *Cannabis sativa* L. *Frontiers in Plant Science*, *15*(June), 1–5. https://doi.org/10.3389/fpls.2024.1412079

Gibson, S. I. (2004). Sugar and phytohormone response pathways: navigating a signalling network. *Journal of Experimental Botany*, *55*(395), 253–264. https://doi.org/10.1093/jxb/erh048

Grassa, C. J., Weiblen, G. D., Wenger, J. P., Dabney, C., Poplawski, S. G., Timothy Motley, S., Michael, T. P., & Schwartz, C. J. (2021). A new Cannabis genome assembly associates elevated cannabidiol (CBD) with hemp introgressed into marijuana. *New Phytologist*, *230*(4), 1665–1679. https://doi.org/10.1111/nph.17243

Guo, Q., Liu, L., Rupasinghe, T. W. T., Roessner, U., & Barkla, B. J. (2022). Salt stress alters membrane lipid content and lipid biosynthesis pathways in the plasma membrane and tonoplast. *Plant Physiology*, *189*(2), 805–826. https://doi.org/10.1093/plphys/kiac123

Hahm, S., Lee, B., Bok, G., Kim, S., & Park, J. (2023). Diniconazole promotes the yield of female hemp (*Cannabis sativa*) inflorescence and cannabinoids in a vertical farming system. *Agronomy*, *13*, 1497. https://doi.org/https://doi.org/10.3390/agronomy13061497

Haider, S., & Pal, R. (2013). Integrated analysis of transcriptomic and proteomic data. *Current Genomics*, *14*(2), 91–110. https://doi.org/10.2174/1389202911314020003

Han, F., & Zhu, B. (2011). Evolutionary analysis of three gibberellin oxidase genesin rice, Arabidopsis, and soybean. *Gene*, *473*(1), 23–35. https://doi.org/10.1016/j.gene.2010.10.010

Hazell, P. B. R. (2009). *The Asian Green Revolution* (Number November 2009).

He, H., Liang, G., Lu, S., Wang, P., Liu, T., Ma, Z., Zuo, C., Sun, X., Chen, B., & Mao, J. (2019). Genome-wide identification and expression analysis of GA2ox, GA3ox, and GA20ox are related to gibberellin oxidase genes in grape (Vitis Vinifera L.). *Genes*, *10*(9), 1–21. https://doi.org/10.3390/genes10090680

Hedden, P. (2003). The genes of the Green Revolution. *Trends in Genetics*, *19*(1), 5–9. https://doi.org/10.1016/S0168-9525(02)00009-4

Hedden, P. (2020). The current status of research on gibberellin biosynthesis. *Plant and Cell Physiology*, *61*(11), 1832–1849. https://doi.org/10.1093/pcp/pcaa092

Hedden, P., & Sponsel, V. (2015). A century of gibberellin research. *Journal of Plant Growth Regulation*, *34*(4), 740–760. https://doi.org/10.1007/s00344-015-9546-1

Helliwell, C. A., Sullivan, J. A., Mould, R. M., Gray, J. C., James Peacock, W., & Dennis, E. S. (2001). A plastid envelope location of Arabidopsis ent-kaurene oxidase links the plastid and endoplasmic reticulum steps of the gibberellin biosynthesis pathway. *Plant Journal*, *28*(2), 201–208. https://doi.org/10.1046/j.1365-313X.2001.01150.x

Hewavitharana, A. K., Gloerfelt-Tarp, F., Nolan, M., Barkla, B. J., Purdy, S., & Kretzschmar, T. (2022). Simultaneous quantification of 17 cannabinoids in Cannabis inflorescence by liquid chromatography-mass spectrometry. *Separations*, *9*(4). https://doi.org/10.3390/separations9040085

Hiremath, S. T., Balasubramanian, S., Zheng, J., & Podila, G. K. (2006). Symbiosis-regulated expression of an acetyl-CoA acetyltransferase gene in the ectomycorrhizal fungus Laccaria bicolor. *Canadian Journal of Botany*, *84*(9), 1405–1416. https://doi.org/10.1139/B06-104

Johnson, N. (2019). American weed: A history of Cannabis cultivation in the United States. *EchoGéo*, *48*, 0–22. https://doi.org/10.4000/echogeo.17650

Kasahara, H., Hanada, A., Kuzuyama, T., Takagi, M., Kamiya, Y., & Yamaguchi, S. (2002). Contribution of the mevalonate and methylerythritol phosphate pathways to the biosynthesis of Gibberellins in Arabidopsis. *Journal of Biological Chemistry*, *277*(47), 45188–45194. https://doi.org/10.1074/jbc.M208659200

Khurshid, T., McNeil, D. L., & Trought, M. C. T. (1997). Effect of foliar-applied gibberellins and soil-applied paclobutrazol on reproductive and vegetative growth of 'Braebum' apple trees growing under a high-density planting system. *New Zealand Journal of Crop and Horticultural Science*, *25*(1), 49–58. https://doi.org/10.1080/01140671.1997.9513986

Langfelder, P., & Horvath, S. (2008). WGCNA: An R package for weighted correlation network analysis. *BMC Bioinformatics*, *9*. https://doi.org/10.1186/1471-2105-9-559

Lemke, C., Potter, K. C., Schulte, S., Peters, R. J., & State, I. (2020). Conserved bases for the initial cyclase in gibberellin biosynthesis: from bacteria to plants. *Biochemical Journal*, *476*(18), 2607–2621. https://doi.org/10.1042/BCJ20190479.Conserved

Livingston, S. J., Rensing, K. H., Page, J. E., & Samuels, A. L. (2022). A polarized supercell produces specialized metabolites in cannabis trichomes. *Current Biology*, *32*(18), 4040-4047.e4. https://doi.org/10.1016/j.cub.2022.07.014

Loreti, E., Povero, G., Novi, G., Solfanelli, C., Alpi, A., & Perata, P. (2008). Gibberellins, jasmonate and abscisic acid modulate the sucrose-induced expression of anthocyanin biosynthetic genes in Arabidopsis. *New Phytologist*, *179*(4), 1004–1016. https://doi.org/10.1111/j.1469-8137.2008.02511.x

Love, M. I., Huber, W., & Anders, S. (2014). Moderated estimation of fold change and dispersion for RNA-seq data with DESeq2. *Genome Biology*, *15*, 550. https://doi.org/doi:10.1186/s13059-014-0550-8

Maier, T., Güell, M., & Serrano, L. (2009). Correlation of mRNA and protein in complex biological samples. *FEBS Letters*, *583*(24), 3966–3973. https://doi.org/10.1016/j.febslet.2009.10.036

Mansouri, H., Asrar, Z., & Mehrabani, M. (2009). Effects of gibberellic acid on primary terpenoids and Δ9 - tetrahydrocannabinol in *Cannabis sativa* at flowering stage. *Journal of Integrative Plant Biology*, *51*(6), 553–561. https://doi.org/10.1111/j.1744-7909.2009.00833.x

Mansouri, H., Asrar, Z., & Szopa, J. (2009). Effects of ABA on primary terpenoids and Δ9-tetrahydrocannabinol in *Cannabis sativa* L. at flowering stage. *Plant Growth Regulation*, *58*(3), 269–277. https://doi.org/10.1007/s10725-009-9375-y

McPartland, J. M., Hegman, W., & Long, T. (2019). Cannabis in Asia: its center of origin and early cultivation, based on a synthesis of subfossil pollen and archaeobotanical studies. *Vegetation History and Archaeobotany*, *28*(6), 691–702. https://doi.org/10.1007/s00334-019-00731-8

McPartland, J. M., & Small, E. (2020). A classification of endangered high-THC cannabis (*Cannabis sativa* subsp. indica) domesticates and their wild relatives. *PhytoKeys*, *144*, 81–112. https://doi.org/10.3897/PHYTOKEYS.144.46700

Micallef, B. J., Haskins, K. A., Vanderveer, P. J., Roh, K.-S., Shewmaker, C. K., & Sharkey, T. D. (1995). Altered photosynthesis, flowering, and fruiting in transgenic tomato plants that have an increased capacity for sucrose synthesis. *Planta*, *196*(2), 327–334.

Mohammad, T., Ghogare, R., Morton, L. B., Dhingra, A., Potlakayala, S., Rudrabhatla, S., & Dhir, S. K. (2024). Evaluation of parameters affecting Agrobacterium-mediated transient gene expression in industrial hemp (*Cannabis sativa* L.). *Plants*, *13*(5). https://doi.org/10.3390/plants13050664

Morikawa, T., Sumiya, M., & Kuriyama, S. (2007). Transfer of new dwarfing genes from the weed species Avena fatua into cultivated oat A. byzantina. *Plant Breeding*, *126*(1), 30–35. https://doi.org/10.1111/j.1439-0523.2007.01309.x

Murcia, G., Pontin, M., & Piccoli, P. (2018). Role of ABA and Gibberellin A3 on gene expression pattern of sugar transporters and invertases in Vitis vinifera cv. Malbec during berry ripening. *Plant Growth Regulation*, *84*(2), 275–283. https://doi.org/10.1007/s10725-017-0338-4

Nagar, S., Singh, V. P., Arora, A., Dhakar, R., Singh, N., Singh, G. P., Meena, S., Kumar, S., & Shiv Ramakrishnan, R. (2021). Understanding the Role of Gibberellic Acid and Paclobutrazol in Terminal Heat Stress Tolerance in Wheat. *Frontiers in Plant Science*, *12*. https://doi.org/10.3389/fpls.2021.692252

Niu, L., Zhang, H., Wu, Z., Wang, Y., Liu, H., Wu, X., & Wang, W. (2018). Modified TCA/acetone precipitation of plant proteins for proteomic analysis. *PLoS ONE*, *13*(12), 1–13. https://doi.org/10.1371/journal.pone.0202238

Nolan, M., Guo, Q., Garcia-de Heer, L., Liu, L., Dimopoulos, N., Barkla, B. J., & Kretzschmar, T. (2025). Bigger is Better; Modern Cannabis Trichomes are Larger and More Productive than their Landrace Ancestors. *Plant and Cell Physiology*, *pcaf105*. https://doi.org/https://doi.org/10.1093/pcp/pcaf105

Nolan, M., Guo, Q., Liu, L., Dimopoulos, N., Garcia-de Heer, L., Barkla, B. J., & Kretzschmar, T. (2025). Characterisation of Cannabis glandular trichome development reveals distinct features of cannabinoid biosynthesis. *Plant Cell Reports*, *44*(30), 1–17. https://doi.org/10.1007/s00299-024-03410-9

Oliveros, J. C. (2015). *Venny. An interactive tool for comparing lists with Venn's diagrams*. Bioinfogp. https://bioinfogp.cnb.csic.es/tools/venny/

Opio, P., Tomiyama, H., Saito, T., Ohkawa, K., Ohara, H., & Kondo, S. (2020). Paclobutrazol elevates auxin and abscisic acid, reduces gibberellins and zeatin and modulates their transporter genes in Marubakaido apple (Malus prunifolia Borkh. var. ringo Asami) rootstocks. *Plant Physiology and Biochemistry*, *155*, 502–511. https://doi.org/10.1016/j.plaphy.2020.08.003

Orozco-Meléndez, L. R., Hernández-Rodríguez, O. A., Cruz-álvarez, O., Robles-Hernández, L., Ávila-Quezada, G. D., Chavez, E. S., Porras-Flores, D. A., & Ojeda-Barrios, D. L. (2022). Paclobutrazol and its use in fruit production: A review. *Phyton-International Journal of Experimental Botany*, *91*(1), 1–12. https://doi.org/10.32604/phyton.2022.016908

Osorio, S., Ruan, Y., & Fernie, A. R. (2014). An update on source-to-sink carbon partitioning in tomato. *Frontiers in Plant Science*, *5*(October), 1–11. https://doi.org/10.3389/fpls.2014.00516

Oultram, J. M. J., Pegler, J. L., Eamens, A. L., Gordon, R., Korbie, D. J., & Grof, C. P. L. (2024). Exogenously applied gibberellic acid alters cannabinoid profile in *Cannabis sativa* L. *Agronomy*, *14*(10). https://doi.org/10.3390/agronomy14102417

Patrick, J. W., & Slewinski, T. L. (2013). Does Don Fisher's high-pressure manifold model account for phloem transport and resource partitioning ? *Frontiers in Plant Science*, *4*(June), 1–17. https://doi.org/10.3389/fpls.2013.00184

Pauwels, L., & Goossens, A. (2011). The JAZ proteins: A crucial interface in the jasmonate signaling cascade. *Plant Cell*, *23*(9), 3089–3100. https://doi.org/10.1105/tpc.111.089300

Pei, G., Chen, L., & Zhang, W. (2017). WGCNA application to proteomic and metabolomic data analysis. *Methods in Enzymology*, *585*, 135–158. https://doi.org/10.1016/bs.mie.2016.09.016

Peng, J., Richards, D. E., Hartley, N. M., Murphy, G. P., Devos, K. M., Flintham, J. E., Beales, J., Fish, L. J., Worland, A. J., Pelica, F., Sudhakar, D., Christou, P., Snape, J. W., Gale, M. D., & Harberd, N. P. (1999). "Green revolution" genes encode mutant gibberellin response modulators. *Nature*, *400*(6741), 256–261. https://doi.org/10.1038/22307

Perazza, D., Vachon, G., & Herzog, M. (1998). Gibberellins promote trichome formation by up-regulating Glabrous1 in arabidopsis. *Plant Physiology*, *117*(2), 375–383. https://doi.org/10.1104/pp.117.2.375

Phengphachanh, B., Naphrom, D., Bundithya, W., & Potapohn, N. (2012). Effects of Day-length and Gibberellic Acid (GA3) on Flowering and Endogenous Hormone Levels in Rhynchostylis gigantea (Lindl.) Ridl. *Journal of Agricultural Science*, *4*(4). https://doi.org/10.5539/jas.v4n4p217

Pingali, P. L. (2012). Green revolution: Impacts, limits, and the path ahead. *Proceedings of the National Academy of Sciences of the United States of America*, *109*(31), 12302–12308. https://doi.org/10.1073/pnas.0912953109

Pri-Tal, O., Sun, Y., Dadras, A., Fürst-Jansen, J. M. R., Zimran, G., Michaeli, D., Wijerathna-Yapa, A., Shpilman, M., Merilo, E., Yarmolinsky, D., Efroni, I., de Vries, J., Kollist, H., & Mosquna, A. (2024). Constitutive activation of ABA receptors in Arabidopsis reveals unique regulatory circuitries. *New Phytologist*, *241*(2), 703–714. https://doi.org/10.1111/nph.19363

Ren, G., Zhang, X., Li, Y., Ridout, K., Serrano-Serrano, M. L., Yang, Y., Liu, A., Ravikanth, G., Nawaz, M. A., Mumtaz, A. S., Salamin, N., & Fumagalli, L. (2021). Large-scale whole-genome resequencing unravels the domestication history of *Cannabis sativa*. *Science Advances*, *7*(29), 1–12. https://doi.org/10.1126/sciadv.abg2286

Rieu, I., Eriksson, S., Powers, S. J., Gong, F., Griffiths, J., Woolley, L., Benlloch, R., Nilsson, O., Thomas, S. G., Hedden, P., & Phillips, A. L. (2008). Genetic analysis reveals that C19-GA 2-oxidation is a major gibberellin inactivation pathway in Arabidopsis. *Plant Cell*, *20*(9), 2420–2436. https://doi.org/10.1105/tpc.108.058818

Rizza, A., & Jones, A. M. (2019). The makings of a gradient: spatiotemporal distribution of gibberellins in plant development. *Current Opinion in Plant Biology*, *47*, 9–15. https://doi.org/10.1016/j.pbi.2018.08.001

Robinson, T. (2011). Advances in apple culture worldwide. *Revista Brasileira de Fruticultura*, *33*(SPEC. ISSUE 1), 037–047. https://doi.org/10.1590/s0100-29452011000500006

RStudio Team. (2020). *RStudio: Integrated Development Environment for R*. RStudio, PBC.

Sands, L. B., Haiden, S. R., Ma, Y., & Berkowitz, G. A. (2023). Hormonal control of promoter activities of *Cannabis sativa* prenyltransferase 1 and 4 and salicylic acid mediated regulation of cannabinoid biosynthesis. *Scientific Reports*, *13*(1), 1–12. https://doi.org/10.1038/s41598-023-35303-4

Sasaki, A., Ashikari, M., Ueguchi-Tanaka, M., Itoh, H., Nishimura, A., Swapan, D., Ishiyama, K., Saito, T., Kobayashi, M., Khush, G. S., Kitano, H., & Matsuoka, M. (2002). A mutant gibberellin-synthesis gene in rice. *Nature*, *416*(6882), 701–702.

Schluttenhofer, C., & Yuan, L. (2017). Challenges towards revitalizing hemp: A multifaceted crop. *Trends in Plant Science*, *22*(11), 917–929. https://doi.org/10.1016/j.tplants.2017.08.004

Si, C. cheng, Li, Y. jie, Liu, H. J., Zhang, H. yan, Meng, Y. yi, Wang, N., & Shi, C. yu. (2023). Impact of paclobutrazol on storage root number and yield of sweet potato (Ipomoea batatas L.). *Field Crops Research*, *300*(April), 109011. https://doi.org/10.1016/j.fcr.2023.109011

Small, E. (2018). Dwarf germplasm: the key to giant Cannabis hempseed and cannabinoid crops. *Genetic Resources and Crop Evolution*, *65*(4), 1071–1107. https://doi.org/10.1007/s10722-017-0597-y

Small, E., & Naraine, S. G. U. (2016). Size matters: evolution of large drug-secreting resin glands in elite pharmaceutical strains of *Cannabis sativa* (marijuana). *Genetic Resources and Crop Evolution*, *63*, 349–359. https://doi.org/10.1007/s10722-015-0254-2

Smith, M. R., Rao, I. M., Merchant, A., & Smith, M. R. (2018). Source-sink relationships in crop plants and their influence on yield development and nutritional quality. *Frontiers in Plant Science*, *9*(December), 1–10. https://doi.org/10.3389/fpls.2018.01889

Song, S., Qi, T., Wasternack, C., & Xie, D. (2014). Jasmonate signaling and crosstalk with gibberellin and ethylene. *Current Opinion in Plant Biology*, *21*, 112–119. https://doi.org/10.1016/j.pbi.2014.07.005

Spitzer, T., & Bílovský, J. (2017). Management of poppy (Papaver somniferum L.) stand height using growth regulators. *Plant Protection Science*, *53*(1), 55–60. https://doi.org/10.17221/24/2016-PPS

Stone, D. (2014). Cannabis, pesticides and conflicting laws: The dilemma for legalized States and implications for public health. *Regulatory Toxicology and Pharmacology*, *69*(3), 284–288. https://doi.org/10.1016/j.yrtph.2014.05.015

Stout, J. M., Boubakir, Z., Ambrose, S. J., Purves, R. W., & Page, J. E. (2012). The hexanoyl-CoA precursor for cannabinoid biosynthesis is formed by an acyl-activating enzyme in *Cannabis sativa* trichomes. *Plant Journal*, *71*(3), 353–365. https://doi.org/10.1111/j.1365-313X.2012.04949.x

Sun, Z., Wang, X., Liu, R., Du, W., Ma, M., Han, Y., Li, H., Liu, L., & Hou, S. (2021). Comparative transcriptomic analysis reveals the regulatory mechanism of the gibberellic acid pathway of Tartary buckwheat (Fagopyrum tataricum (L.) Gaertn.) dwarf mutants. *BMC Plant Biology*, *21*(1), 1–17. https://doi.org/10.1186/s12870-021-02978-8

Symons, G. M., Smith, J. J., Nomura, T., Davies, N. W., Yokota, T., & Reid, J. B. (2008). Brassinosteroids, de-etiolation and the re-emerging art of plant hormone quantification. *Plant Signaling and Behavior*, *3*(10), 868–870. https://doi.org/10.1007/s00425-007-0685-x

Tamura, K., Stecher, G., & Kumar, S. (2021). MEGA11: Molecular Evolutionary Genetics Analysis Version 11. *Molecular Biology and Evolution*, *38*(7), 3022–3027. https://doi.org/10.1093/molbev/msab120

Tang, L., Ma, W., Noor, M. A., Li, L., Hou, H., Zhang, X., & Zhao, M. (2018). Density resistance evaluation of maize varieties through new "Density–Yield Model" and quantification of varietal response to gradual planting density pressure. *Scientific Reports*, *8*(1), 1–16. https://doi.org/10.1038/s41598-018-35275-w

Thomas, S. G., Phillips, A. L., & Hedden, P. (1999). Molecular cloning and functional expression of gibberellin 2-oxidases, multifunctional enzymes involved in gibberellin deactivation. *Proceedings of the National Academy of Sciences of the United States of America*, *96*(8), 4698–4703. https://doi.org/10.1073/pnas.96.8.4698

Tissier, A., Morgan, J. A., & Dudareva, N. (2017). Plant Volatiles: Going 'In' but not 'Out' of Trichome Cavities. *Trends in Plant Science*, *22*(11), 930–938. https://doi.org/10.1016/j.tplants.2017.09.001

Unkovich, M., Baldock, J., & Forbes, M. (2010). Variability in harvest index of grain crops and potential significance for carbon accounting: Examples from Australian agriculture. In *Advances in Agronomy* (1st ed., Vol. 105, Number 10). Elsevier Inc. https://doi.org/10.1016/S0065-2113(10)05005-4

Upreti, K. K., Reddy, Y. T. N., Prasad, S. R. S., Bindu, G. V., Jayaram, H. L., & Rajan, S. (2013). Hormonal changes in response to paclobutrazol induced early flowering in mango cv. Totapuri. *Scientia Horticulturae*, *150*, 414–418. https://doi.org/10.1016/j.scienta.2012.11.030

Vogel, C., & Marcotte, E. M. (2012a). Insights into the regulation of protein abundance from proteomic and transcriptomic analyses. *Nature Reviews Genetics*, *13*(4), 227–232. https://doi.org/10.1038/nrg3185

Vogel, C., & Marcotte, E. M. (2012b). Insights into the regulation of protein abundance from proteomic and transcriptomic analyses. *Nature Reviews Genetics*, *13*(4), 227–232. https://doi.org/10.1038/nrg3185

Wang, X., Liu, Q., & Zhang, B. (2014). Leveraging the complementary nature of RNA-Seq and shotgun proteomics data. In *Proteomics* (Vol. 14, Numbers 23–24, pp. 2676–2687). Wiley-VCH Verlag. https://doi.org/10.1002/pmic.201400184

Wang, Y., Yu, W., Li, S., Guo, D., He, J., & Wang, Y. (2022). Acetyl-CoA Carboxylases and Diseases. *Frontiers in Oncology*, *12*(March), 1–10. https://doi.org/10.3389/fonc.2022.836058

Weijers, D., & Wagner, D. (2016). Transcriptional Responses to the Auxin Hormone. In *Annual Review of Plant Biology* (Vol. 67, pp. 539–574). Annual Reviews Inc. https://doi.org/10.1146/annurev-arplant-043015-112122

Weiss, D., & Ori, N. (2007). Mechanisms of cross talk between gibberellin and other hormones. *Plant Physiology*, *144*(3), 1240–1246. https://doi.org/10.1104/pp.107.100370

Welling, M. T., Deseo, M. A., O'Brien, M., Clifton, J., Bacic, A., & Doblin, M. S. (2023). Metabolomic analysis of methyl jasmonate treatment on phytocannabinoid production in *Cannabis sativa*. *Frontiers in Plant Science*, *14*(March), 1–16. https://doi.org/10.3389/fpls.2023.1110144

Westerhuis, W., van Delden, S. H., van Dam, J. E. G., Pereira Marinho, J. P., Struik, P. C., & Stomph, T. J. (2019). Plant weight determines secondary fibre development in fibre hemp (*Cannabis sativa* L.). *Industrial Crops and Products*, *139*(June), 111493. https://doi.org/10.1016/j.indcrop.2019.111493

White, A. C., Rogers, A., Rees, M., & Osborne, C. P. (2016). How can we make plants grow faster? A source–sink perspective on growth rate. *Journal of Experimental Botany*, *67*(1), 31–45. https://doi.org/10.1093/jxb/erv447

Wickham, H. (2016). *ggplot2: Elegant Graphics for Data Analysis*. Springer-Verlag New York.

Wu, H., Chen, H., Zhang, Y., Zhang, Y., Zhu, D., & Xiang, J. (2019). Effects of 1-aminocyclopropane-1-carboxylate and paclobutrazol on the endogenous hormones of two contrasting rice varieties under submergence stress. *Plant Growth Regulation*, *87*(1), 109–121. https://doi.org/10.1007/s10725-018-0457-6

Wu, T., Hu, E., Xu, S., Chen, M., Guo, P., Dai, Z., Feng, T., Zhou, L., Tang, W., Zhan, L., Fu, X., Liu, S., Bo, X., & Yu, G. (2021a). clusterProfiler 4.0: A universal enrichment tool for interpreting omics data. *The Innovation*, *2*(3), 100141. https://doi.org/10.1016/j.xinn.2021.100141

Wu, T., Hu, E., Xu, S., Chen, M., Guo, P., Dai, Z., Feng, T., Zhou, L., Tang, W., Zhan, L., Fu, X., Liu, S., Bo, X., & Yu, G. (2021b). clusterProfiler 4.0: A universal enrichment tool for interpreting omics data. *The Innovation*, *2*(3), 100141. https://doi.org/10.1016/j.xinn.2021.100141

Xiang, J., Wu, H., Zhang, Y., Zhang, Y., Wang, Y., Li, Z., Lin, H., Chen, H., Zhang, J., & Zhu, D. (2017a). Transcriptomic analysis of gibberellin- and paclobutrazol-treated rice seedlings under submergence. *International Journal of Molecular Sciences*, *18*(10). https://doi.org/10.3390/ijms18102225

Xiang, J., Wu, H., Zhang, Y., Zhang, Y., Wang, Y., Li, Z., Lin, H., Chen, H., Zhang, J., & Zhu, D. (2017b). Transcriptomic analysis of gibberellin- and paclobutrazol-treated rice seedlings under submergence. *International Journal of Molecular Sciences*, *18*(10). https://doi.org/10.3390/ijms18102225

Yano, K., Aya, K., Hirano, K., Ordonio, R. L., Ueguchi-Tanaka, M., & Matsuoka, M. (2015). Comprehensive gene expression analysis of rice aleurone cells: Probing the existence of an alternative gibberellin receptor. *Plant Physiology*, *167*(2), 531–544. https://doi.org/10.1104/pp.114.247940

Yeo, H. C., Reddy, V. A., Mun, B. G., Leong, S. H., Dhandapani, S., Rajani, S., & Jang, I. C. (2022). Comparative transcriptome analysis reveals coordinated transcriptional regulation of central and secondary metabolism in the trichomes of Cannabis cultivars. *International Journal of Molecular Sciences*, *23*(15). https://doi.org/10.3390/ijms23158310

Yu, G., Smith, D. K., Zhu, H., Guan, Y., & Lam, T. T. Y. (2017). Ggtree: an R package for visualization and annotation of phylogenetic trees with their covariates and other associated data. *Methods in Ecology and Evolution*, *8*(1), 28–36. https://doi.org/10.1111/2041-210X.12628

Yu, W., Peng, F., Wang, W., Liang, J., Xiao, Y., & Yuan, X. (2021). SnRK1 phosphorylation of SDH positively regulates sorbitol metabolism and promotes sugar accumulation in peach fruit. *Tree Physiology*, *41*(6), 1077–1086. https://doi.org/10.1093/treephys/tpaa163

Zhang, C., Nie, X., Kong, W., Deng, X., Sun, T., Liu, X., & Li, Y. (2022). Genome-Wide Identification and Evolution Analysis of the Gibberellin Oxidase Gene Family in Six Gramineae Crops. *Genes*, *13*(5), 1–16. https://doi.org/10.3390/genes13050863

Figure Legends

Figure 1. Floral phenotype and plant stature of treated clones (n=6). Plants were treated with 200 ppm gibberellic acid (GA3), distilled water (Control) or 50 ppm paclobutrazol (PBZ), on days 26, 28 and 30 of the experiment. Treatments resulted in taller plants with smaller inflorescences for GA3, while PBZ reduced plant height resulting in more compact inflorescences. Photos taken 28 days into the flowering period.

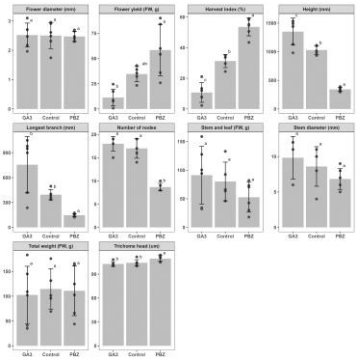

Figure 2. Agronomic parameters of GA3, Control and PBZ treatment groups (n=6). Measured at harvest after 6 weeks of flowering (Day 70). Error bars represent standard deviation. ANOVA with Tukey-post hoc analysis were performed to identify significantly different treatment groups (P<0.05) (Supplementary Tables S3, S4 and S6).

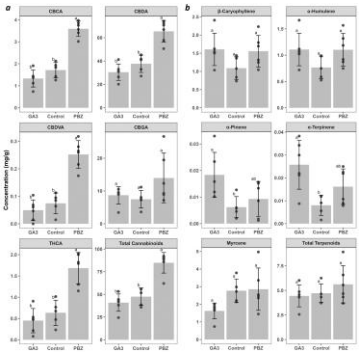

Figure 3. Comparison of secondary metabolite profiles of GA3, Control and PBZ treatment groups (n=6). Quantified from dried flower material collected at harvest after 6 weeks of flowering (Day 70) of A) five most abundant cannabinoids cannabichromenic acid (CBCA), cannabidiolic acid (CBDA), cannabidivarinic acid (CBDVA), cannabigerolic acid (CBGA) and tetrahydrocannabinolic acid and B) five most abundant terpenoids β-caryophyllene, α-humulene, α-pinene, α-terpinene, and myrcene (THCA) (mg/g). Error bars represent standard deviation. One-way ANOVA with Tukey-post hoc analysis were performed with letters to identify significantly different treatment groups (Supplementary Table S5).

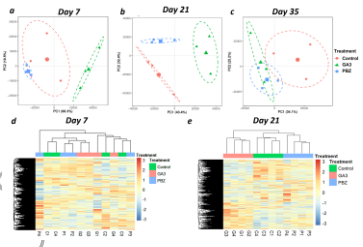

Figure 4. Sample clustering in proteomic and transcriptomic data in GA3, Control and PBZ treatment groups. A-C) Principal Component Analysis of floral proteomes at three time points 7 (A), 21 (B) and 35 (C) days into flowering (n=3). D-E) Hierarchical cluster of transcript expression at two time points, 7 (D) and 21 (E) days into flowering (n=4). Clear separation of treatment groups at day 21 in both –omics datasets led to the

focus of this timepoint in further analysis. Refer to Supplementary Table S7 for protein abundance and Table S8 for DEG designations when p.adjust<0.01 and log2foldchange>1.

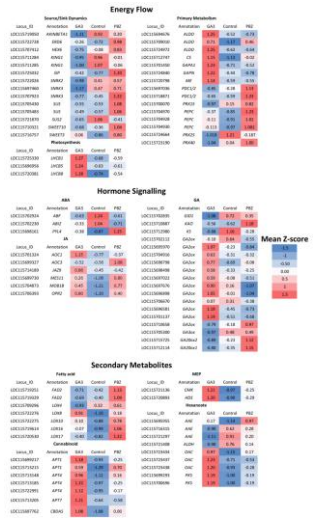

Figure 5. Heatmap profiles of DEGs of interest in energy flow, hormone signalling and secondary metabolite related pathways. Mean z-score of median of ratios normalised transcript counts are shown for GA3, Control and PBZ treatment groups. All transcripts have mean normalised counts >50. Refer to Supplementary Table S12 for sample z-scores and CBDRx transcript IDs.

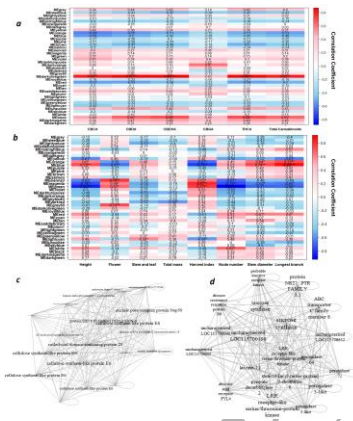

Figure 6. Weighted correlation network analysis of floral transcriptomes 21 days into flowering. A) Module – cannabinoid content (mg/g) associations. B) Module – agronomic trait associations. Rows refer to a module eigengenes, and columns to individual morphological traits or cannabinoid content. Heatmap asterisks refer to significance, p<0.001 = ***, p<0.01 = **, p<0.05 = *. C) 20 most connected genes in the dark olive green module D) 20 most connected genes in the magenta module. CBDRx descriptions used as node labels, and size based on gene within module connectivity. Refer to Supplementary Table S14 for individual trait correlations, Supplementary Table S13 for top dark olive green and magenta transcripts.

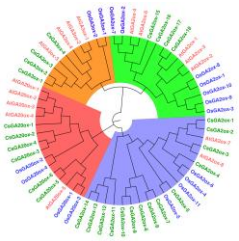

Figure 7. Phylogenetic analysis of putative GAox proteins in *C sativa*. A phylogenetic tree was constructed using 16 Arabidopsis thaliana (red) and 17 Ozyra sativa (blue) seed sequences, with 28 putative *Cannabis sativa* (green) proteins being identified (Supplementary Table S16). Branch colouring refers to sub-family designation, with GA3ox (yellow), GA2ox (green and blue), and GA20ox (red). Seed sequences were used to BLASTP query (E-value cut off of e-10) the *C. sativa* protein dataset, before sequences were screened to ensure they contained 2OG-FeII_Oxy (PF03171) and DIOX_N (PF14226) domains. Multi-sequence alignments and phylogenetic trees of candidate proteins were performed to remove proteins that did not cluster with seed GAox proteins. Refer to Supplementary Figure S8 for motif analysis.